Published in final edited form as:
Acta Biomater. 2014 February ; 10(2): 742–750. doi:10.1016/j.actbio.2013.10.018.

Microfluidic Fabrication of MEAN-Eluting Magnetic Microspheres

Dong-Hyun Kim[a,g,*], **Terence Choy**[a], **Sui Huang**[b], **Richard M Green**[c], **Reed A. Omary**[d], and **Andrew C. Larson**[a,e,f,g,h,i]

[a]Department of Radiology, Northwestern University, Chicago, IL, USA

[b]Department of Cell and Molecular Biology, Northwestern University Feinberg School of Medicine Chicago, IL, USA

[c]Division of Hepatology, Northwestern University Feinberg School of Medicine Chicago, IL, USA

[d]Department of Radiology and Radiological Sciences, Vanderbilt University Medical Center, Nashville, TN, USA

[e]Department of Bioengineering, University of Illinois at Chicago, Chicago, IL, USA

[f]Department of Electrical Engineering and Computer Science, Evanston, IL, USA

[g]Robert H. Lurie Comprehensive Cancer Center, Chicago, IL, USA

[h]Department of Biomedical Engineering, Northwestern University, Chicago, IL, USA

[i]International Institute of Nanotechnology (IIN), Northwestern University, Evanston, IL, USA

Abstract

Recently, 6-methoxyethylamino numonafide (MEAN) exhibited potent inhibition of hepatocellular carcinoma (HCC) cell growth and less systemic toxicity than amonafide. MEAN may serve as an ideal candidate for the treatment of HCC; however, liver-directed, selective infusion methods may be critical to maximize MEAN dose delivered to the targeted tumors. Our study describes the microfluidic fabrication of MEAN-eluting ultrasmall superparamagnetic iron oxide (USPIO) nanocluster-containing alginate microspheres (MEAN-magnetic microspheres) intended for selective transcatheter delivery to hepatocellular carcinoma. The resulting drug delivery platform was mono-disperse, microsphere sizes were readily controlled based upon channel flow rates during synthesis procedures, and drug release rates from the microspheres could be readily controlled with the introduction of USPIO nanoclusters. The MR relaxivity properties of the microspheres suggest the feasibility of *in vivo* imaging after administration and these microspheres exhibited potent therapeutic effects significantly inhibiting cell growth inducing apoptosis in hepatoma cells.

INTRODUCTION

Hepatocellular carcinoma (HCC) is among the 10 most common neoplasms worldwide and the third most common cause of cancer-related death.[1] Surgical resection remains the only

*Corresponding author: Department of Radiology, Northwestern University Feinberg School of Medicine, 710 N Fairbanks Ct. Olson 8-317, Chicago, IL 60611, USA. Tel.: 1-312-503-1307; Fax: 1-312-926-5991 dhkim@northwestern.edu and dhkim0405@gmail.com (D.-H. Kim).

curative treatment for HCC. However, resection is feasible in only 25–30% of patients due to tumor stage or the severity of underlying cirrhosis. Systemic doxorubicine chemotherapy or a combination of doxorubicin with cisplatin and mitomycin C offers limited survival benefits with serious side effects such as pain, nausea, vomiting, myelosuppression, and alopecia as well as cardiac toxicity that may be life-threatening.[2] Loco-regional therapies such as transcatheter arterial chemoembolization (TACE) involve image-guided placement of infusion catheters for selective intra-arterial delivery of chemotherapeutic agents to the targeted liver tumors. TACE can reduce systemic toxicities and improve survival due to preferential drug delivery to liver tumors (hepatic arteries supply ~90% of blood flow to HCC).[3–6] TACE approaches have resulted in a modest improvement in HCC patient survival but a complete response is achieved in only 35% of patients.[7] Overall prognosis of these patients remains poor[7, 8.]

Amonafide is an anti-neoplastic agent that acts as a DNA intercalator; amonafide has demonstrated significant activity against a broad range of solid tumors.[9–11] However, amonafide has a 5-position amine that is acetylated to form a toxic metabolite (N-acetyl metabolite) causing potentially serious adverse events, complicating dosing, and ultimately limiting clinical utility. Recently, a less toxic form was developed, 6-meth-oxyethylamino numonafide (MEAN). MEAN retains the anti-cancer effects of amonafide while not generates toxic metabolites with a protected amine. MEAN is chemically similar to amonafide thus retaining potency, selectivity and similar biological activity. During recent *in vitro and in vivo* studies in HCC mouse models,[12, 13] MEAN exhibited potent inhibition of tumor cell growth and less toxicity than amonafide. MEAN may serve as an ideal candidate for the treatment of HCC; however, liver-directed, selective infusion methods may be critical to maximize MEAN dose delivered to the targeted tumors.

Recently developed catheter-directed infusion approaches utilize drug-eluting beads as opposed to conventional TACE methods wherein drugs are administered after emulsification within iodinated oils. Selective infusion and sustainable, controlled drug release should offer significant therapeutic benefits. However, arterially administered microspheres can also result in tissue ischemia, cholecystitis, liver abscesses or infarction due to sub-optimal microsphere sizes and resulting distribution volumes. Conventional microsphere fabrication techniques commonly yield microspheres with broad distributions in size due to the inhomogeneous forces involved in the synthesis process. Broad distributions in size and morphology along with quality discrepancies within and between different batches may result in unpredictable biodistributions distal to the infusion catheter, variable degradation rates and associated variable kinetics of drug release. To date, a broad range of strategies such as atomization, coacervation and emulsification for the generation of drug eluting microspheres/beads exist; these methods involve multistage processes, often do not utilize biocompatible components or do not allow precise control of the dimensions and internal structure of the drug eluting carriers. Microfluidic techniques of continuous synthesis and fabrication for the production of drug eluting composite carriers now offer precise control over the shapes, morphologies, and size distributions of composite colloids. Microfluidic droplet generation primarily involves shearing of one liquid into a second immiscible fluid. The streams operate in the laminar flow regime, thereby permitting precise control over micro-spherical droplet properties compared to more conventional techniques such as atomization, coacervation, and emulsification.

Alginate biopolymers may be an ideal material for preparation of drug delivery microspheres with low toxicity, biocompatibility and the ability to degrade. The biodegradable polysaccharide alginate has attracted attention as an important class of biomaterials due to a relatively inert hydrogel environment within the matrix and a mild room-temperature encapsulation process. Alginate has been extensively investigated for

many biomedical applications serving as a key component of engineered tissues, drug delivery vehicles, and cell transplantation matrices.[14–18] Microspheres derived from alginate are attractive for a broad range of applications owing to their low toxicity, biocompatibility and ability to degrade due to the action of various biological stimuli. The amount of chemotherapy loaded into these microspheres and associated drug release rates can be precisely controlled. Microfluidic fabrication techniques should permit highly controlled formation of alginate microspheres at micrometer size scales. Droplet microfluidic methods have proven effective for the generation of mono-dispersed Ca-alginate microspheres with highly controlled sizes, morphologies, and size distributions.[19] Importantly, biopolymer materials such as alginate can be blended with inorganic nanoparticles or other polymers and/or grafted with monomers, to improve drug loading efficiency and drug release behavior.[20–22] USPIO (ultrasmall superparamagnetic iron oxide) nanoparticles serving in this role should concurrently permit *in vivo* detection with magnetic resonance imaging (MRI). Imaging microsphere biodistribution after transcatheter infusion might prove invaluable for timely prediction of tumor response in individual patients.

Our current study describes the microfluidic fabrication of MEAN-eluting USPIO nanocluster-containing alginate microspheres (MEAN-magnetic microspheres) intended for selective transcatheter delivery to HCC. The morphologic characteristics of these fabricated microspheres (shape, size distribution) were rigorously characterized prior to subsequent drug loading and release studies. Finally, *in vitro* studies were performed to validate the potential to elicit potent therapeutic responses upon exposure of HCC cells to our MEAN-eluting microspheres.

MATERIALS AND METHODS

Synthesis of 6-Methoxyethylamino Numonafide (MEAN)

MEAN was synthesized as reported in previous publications.[12, 13] Briefly, 6-nitro-imide precursor (200 mg, 0.64 mmol) and excess 2-methoxyethylamine (0.5 ml) in DMF (1 ml) were reacted to yield 33.8 mg (15.5%) of MEAN as a bright orange solid. Proton nuclear magnetic resonances (^{1}H-NMRs) were recorded in deuterated solvents on a Gemini 300 (300MHz; Varian, Palo Alto, California, USA) or an iNOVA 500 (500 MHz; Varian) spectrometer. Mass spectra were obtained using an API 3000 LC/MS/MS system (Applied Biosystems, Foster City, California, USA), a Micromass Quattro II Triple Quadrupole HPLC/MS/MS mass spectrometer (Waters, Milford, Massachusetts, USA) or a Waters LCT Premier time-of- flight mass spectrometer (Waters). The spectral characteristics of MEAN were measured with UV/vis and fluorescent spectroscopy (SpectraMax M5, Molecular Devices, CA, USA).

Synthesis of USPIO Nanoclusters and Characterization of MR Relaxivity

Ferric chloride ($FeCl_3$), diethylene glycol (DEG), sodium hydroxide, poly acrylic acid (PAA) were purchased from Sigma-Aldrich. USPIO nanoclusters were synthesized using a high temperature hydrolysis reaction.[23] Briefly, a NaOH/DEG stock solution was prepared by dissolving 2 g of NaOH in diethylene glycol (DEG) (20 ml). The solution was heated to 120 °C for 30 mins under nitrogen, cooled, and kept at 70°C. A mixture of $FeCl_3$ (0.4 mmol), polyacrylic acid (PAA) (4 mmol), and DEG (17 ml) was heated to 220 °C in a nitrogen atmosphere for 30 min with vigorous stirring to form a transparent solution. NaOH/DEG stock solution (2 ml) was injected into the hot mixture. The resulting mixture was further heated for 1 h to yield ~42 nm USPIO nanoclusters composed by ~6 nm USPIO. The final product was precipitated by addition of excess of a mixture of Milli-Q water/ethanol and collected by centrifugation (3,500 rpm, 10 min, room temperature). The nanoparticles were repeatedly washed by precipitating them with Milli-Q water/ethanol and centrifugation

(3,500 rpm, 10 min, room temperature). Finally, the product was re-dispersed in Milli-Q water. MR relaxivities of the USPIO clusters were investigated using a 7 Tesla MRI scanner (BioSpec, Bruker, Billerica, MA, USA). Imaging phantoms were prepared by diluting samples in 0.1% agarose at various particle concentrations. The atomic Fe concentrations of the stock solutions were determined using Inductively Coupled Plasma Spectroscopy (Inductively Coupled Plasma Mass Spectrometer (ICP-MS), Perkin Elmer, Waltham, MA, USA).

Microfluidic Fabrication of Magnetic Microspheres

Microfluidic chips with a channel dimension of 120 um in depth and width were fabricated by soft lithography techniques (Fig. 3). The microfluidic chips were molded with a mixture of PDMS elastomer base/curing agent in 10:1 ratio from SU-8 mold and bonded to a flat PDMS substrate under plasma treatment for 90 s. A two-step droplet gelation process was adopted to produce MEAN-magnetic microspheres. Oil used as the continuous phase was composed of n-hexadecane and span 80 (2% w/w). Aqueous solutions of sodium alginate (2% w/w), USPIO clusters and MEAN were prepared for the dispersed phase. All flow streams were individually driven using independent syringe pumps (New Era NE-1000, NY, USA) to maintain a constant flow rate. The inlet ports were connected to the syringes (20 ml) using Tygon tubing (.02 inch I.D). A microscope equipped with a variable zoom system was used for observation (Olympus, Japan). As shown in Fig. 3, these two fluids were supplied into the microfluidic channels using the syringe pumps. The dispersed phase stream was broken up to generate droplets due to the shear force imposed by the oil continuous phase in-flow focusing channel. These droplets were collected in calcium chloride (50mM; 20 ml) reservoir for external gelation experiments. Once the droplets were dripped into the calcium chloride solution, the MEAN loaded magnetic alginate droplets were solidified. The amount of USPIO clusters included in the dispersed phase was varied from 0 to 5 wt% relative to the amount of alginate material. The resulting MEAN-magnetic microspheres were separated from the oil solution via centrifuge. These were subsequently washed twice with 30 mL of Milli-Q water and permanent magnet. Finally, the microspheres were dried at room temperature. The size, morphology, and magnetic properties of these synthesized microspheres were characterized with an optical microscope, scanning electronic microscope, confocal laser-scanning microscope and superconducting quantum interface device (SQUID), respectively. Size distributions were determined by examination of randomly selected 300 microsphere samples. The fluorescent properties of these MEAN-magnetic microspheres were measured with UV/vis and fluorescent spectroscopy. Degradation of the microspheres was evaluated using a method described by Schwarz et al. (A.Schwarz,et al., Biomaterials 25(2004) 5209–5215.)

Drug Loading Efficiency and Drug Release Studies

MEAN loading efficiency in each sample was measured after microsphere solubilization in a 50 mM ethylenediaminetetraacetic acid (EDTA) solution with sonication for 10 mins. Released MEAN drug was quantified based upon characteristic fluorescence emissions at a wavelength of 550 nm following excitation at 445 nm. Results were expressed as a percentage relative to the initial feeding amount of MEAN during the microfluid fabrication processes. These determinations were carried out in triplicate for each formulation. Drug elution studies for each set of microspheres were performed to compare MEAN release kinetics for microspheres incorporating different amounts of the USPIO clusters (0~5 wt%) at 37 °C. An aqueous sample solution (10 mg/ml;1 ml) was placed into a membrane bag (Spectra/Por MWCO 10,000, Spectrum, Los Angeles, CA, USA) and then immersed in 40 ml of PBS (Phosphate Buffer Solution, pH 7.2). The temperature of the medium was maintained at 37 °C using a water bath. At specific time intervals, PBS medium (1 ml) was extracted and replaced with fresh medium. The concentration of released MEAN within

these samples was determined using fluorescent spectroscopy (SpectraMax M5, Molecular Devices, CA, USA). These measurements were performed three times and averaged to determine percentages of cumulative drug release over the time.

In vitro Exposure of McA-RH7777 Hepatoma Cells to MEAN-Magnetic Microspheres

A McA-RH7777 hepatoma cell line (ATCC, CRL-1601, Manassas, VA, USA) was cultured in Dulbecco's Modified Eagle's Medium (DMEM, ATCC, Manassas, VA, USA) supplemented with 10% fetal bovine serum (Sigma-Aldrich, MO, USA) and 0.1% gentamycin (Sigma-Aldrich, MO, USA). Cells from the exponential phase of the culture were harvested and diluted to a cell density of about 2×10^4 per ml. 100 μl of the cell suspension was added to 180 μl of medium in each well of a 96-well plate, incubated at 37 °C, 5% CO_2 and 95% air for 1 day. A 100 μl solution consisting of different amounts of either free MEAN or MEAN-magnetic microspheres was then added to the respective wells and incubated for specific periods of time. Studied concentrations of MEAN (within either free MEAN or MEAN-magnetic microsphere doses) ranged from 1.25 to 50 μM. Control studies were conducted by dose wells with normal saline without MEAN drug or MEAN-magnetic microspheres. Exposure time was varied from 8 to 40 h. Treated cells were then rinsed with PBS before 20 μl of PBS consisting of 5 mg/ml of MTT was added prior to incubation for another 4 h. This was followed by the addition of 150 μl of DMSO and plate agitation for 10 min. The optical density (OD) of the contents in each well was then measured at 570 nm using a bioassay reader (SpectraMax M5, Molecular Devices, CA, USA). OD measurements were repeated in triplicate. The growth inhibitory (GI) effect was calculated as follows, $\mathrm{GI}=(\mathrm{OD}_{\mathrm{control}}-\mathrm{OD}_{\mathrm{test}})/\mathrm{OD}_{\mathrm{control}}{}^{*}100$, where $\mathrm{OD}_{\mathrm{test}}$ and $\mathrm{OD}_{\mathrm{control}}$ are the mean OD values for medium solutions with and without MEAN dosing, respectively. The toxicity of the magnetic microspheres was also evaluated with MTT assay. For dose dependent cell growth inhibition plots, the half maximal inhibitory concentration (IC50) was calculated for each sample. Apoptosis and necrosis were determined by propidium iodide and Annexin-V-Fluos (Roche Molecular Biochemicals) as previously described.[24] For cell death analysis, McA-RH7777 cells were treated with increasing MEAN concentrations (12.5, 30, and 50 uM) for 24 h and were analyzed with FACS (Becton Dickinson LSRFortessa flow cytometer). The percentage of necrotic cells (propidium iodide–positive annexin-positive), and apoptotic cells (propidium iodide-annexin-positive) were determined. Data were collected using CellQuest software (BD Biosciences) and analyzed using FCS Express (De Novo Software).

RESULTS AND DISCUSSION

MEAN (6-methoxyethylamino numonafide)

MEAN was synthesized and chemical structure confirmed as described previously with ^{1}H-NMR[13] (Fig. 1a). MEAN is visibly orange-yellow in color with fluorescence spectra displaying a distinguished absorption peak at 455 nm (Fig. 1b). Emission spectra at 552 nm were measured upon excitation at 455 nm for solutions with increasing concentrations of the drug (Fig. 1c); fluorescent intensity clearly increased with increasing MEAN content within the solutions. The spectral characteristics of MEAN may be particularly useful for measuring MEAN concentrations within dilute suspensions of unknown composition or potentially for monitoring the biodistribution in MEAN-loaded microspheres.

MEAN-Magnetic Microspheres Fabricated with Droplet Microfluidics

USPIO nanoclusters (~42 nm in size) were formed by polyacrylic acid coupling among 6 nm USPIO nanoparticles (Fig. 2a and 2b). USPIO nanocluster solutions were strongly water-dispersible and stable in aqueous solution with a surface charge of −48.7 mV (zetapotential) caused by dissociation of the characteristic carboxylic acid on the clusters.

The measured hydrodynamic size (45±2 nm) and zetapotential were not changed during 1-month storage at 4 degree C. These synthesized USPIO clusters demonstrated 3 times higher r_2 relaxivity (302 $mM^{-1}s^{-1}$) than non-clustered 6 nm USPIO nanoparticles. Given stable aqueous dispersion, strong r_2 relaxivity, and biocompatible constituents, these anionic PAA coated USPIO clusters should be ideal to serve as functional components in drug delivery vehicles and/or MR contrast agents. For our study, these USPIO clusters were incorporated into an alginate microsphere drug delivery platform permitting controlling drug release and the potential for MRI visualization upon delivery. Microfluidic methods were effective for the synthesis of alginate microspheres encapsulating both MEAN and USPIO clusters. Resulting microsphere sizes (ranging from 30–73 um) were dependent upon flow rates of dispersed and continuous phase channels. During the fabrication process, a pre-gel solution (20 mL of 2% w/v alginate solution and pre-mixed MEAN and USPIO clusters solution) and n-hexadecane with SPAN 80 (2 % w/v) as a respective dispersed-phase fluid (dispersed flow) and continuous-phase fluid (continuous oil flow) were fed into the prepared PDMS microfluidic chip (Fig. 3). As soon as the dispersed-phase was fed into a flow-focusing region, it was sheared by the two continuous oil phase streams, instantly forming droplets (Fig. 3). Flow rates of the dispersed and continuous phase solutions were adjusted to control the focusing and width of the center stream, controlling the size of resulting droplets (Fig. 4a). The continuous oil phase mixed with SPAN 80 prevented the pre-gel droplets from fusing together transporting the droplets stably to a 5% calcium chloride aqueous pool through a Teflon tube. Importantly, SPAN 80 concentration had a significant impact upon the stability of droplet generation. During these studies it was difficult to stably generate monodisperse droplets when the concentration of SPAN 80 was less than 0.5% and the collected droplets tended to fuse together when the concentration of SPAN 80 was less than 1.5%. 2% SPAN80 was optimal stabilizing and inhibiting coalescence of the droplets. Fig. 4 shows the relationship between droplet size and the flow rates of the dispersed and continuous phases. Diameters of the droplets increased with increasing flow rates of dispersed phase solution, Q_d or decreasing flow rate of the continuous oil phase, Q_c (Fig. 4a and 4b). By changing the values of Q_c from 3 to 45 uL/min and Q_d from 0.5 to 7 uL/min, we obtained alginate droplets with diameters from 30 to 73 μm and polydispersities of ~4 %. The relationship between flow rate and droplet size was well described by the equation $Q_c = D_d Q_d$ (under dynamic balance), where Q_c is the flux of the dispersed phase, D_d is the size of the droplets, and Q_d is the flow rate of the dispersed phase.[25] For a fixed flow rate of the dispersed phase (Q_d=1 ul/min), the droplet size decreased as the flow rate of the continuous phase increased from 5 ul/min to 15 ul/min (Fig. 4c). These size-controlled droplets in a microfluidic channel were gelled into solid microspheres upon contact with $CaCl_2$ by crosslinking, producing MEAN-magnetic microspheres (Fig. 5). Liberated calcium ions in the $CaCl_2$ solution bind to the a-l-guluronic residues of sodium alginate, crosslinking the polymer and causing gelation of the droplets. The shape of the microspheres remained spheroid after the crosslinking gelation (Fig. 5). The size of the cross-linked microspheres decreased in diameter by ~8% compared to the original droplet sizes. For MEAN release and *in vitro* cell exposure tests (*see below*), 43 um MEAN-magnetic microspheres were synthesized setting flow rates of the dispersed phase to 1 uL/min and the continuous phase to 15 uL/min, respectively (Fig. 5). The measured average diameter of these microspheres was 43 um with a size variation of only 4%. The highly uniform size distribution permissible with these microfluidic fabrication techniques should be particularly valuable for the production of microspheres intended for intra-arterial transcatheter delivery. The size of the microspheres importantly determines the distance within the vascular tree, distal to the infusion catheter tip, transversed by microspheres which ultimately lodge within the capillary bed potentially blocking forward blood flow. Depending upon the particular application, interventional radiologists generally desire strict control over the resulting biodistribution of administered microspheres thus rigorously controlling the size of the

microspheres may be particularly valuable. In addition, agar phantom signal intensities in MR imaging changed with increasing concentration of magnetic microspheres (Fig. 6). For the 5 magnetic microspheres concentrations, T2*-weighted images demonstrated the potential benefits of visibility with MR imaging (Fig. 6).

MEAN Loading and Release Rates

Both MEAN and USPIO nanoclusters were effectively loaded into the alginate microspheres. Drug loading efficiencies improved with the addition of USPIO nanoclusters. The drug loading efficiency ranged from 54% to 75% with co-encapsulation of 0 to 5 wt% USPIO nanoclusters, respectively. Fluorescent images demonstrated that MEAN was dispersed throughout the microspheres (Fig. 7a and 7b). However, intense punctate spikes of fluorescence intensity were observed within regions of condensed USPIO nanoclusters suggesting increased concentrations of the drug at these positions within the microspheres.

Co-encapsulation of USPIO nanoclusters clearly altered resulting MEAN release kinetics (Fig. 8). For microspheres without USPIO nanoclusters, 76% of the drug was released within the first 8 hours. Co-encapsulating USPIO nanoclusters significantly slowed release rates such that only 56, 43, and 36% of the drug was released within the first 8 hrs for microspheres including 1, 3, and 5 wt% USPIO nanoclusters, respectively. When we extended the periods of drug release, the magnetic microspheres of 3wt% and 5wt% USIPO released most of the drug (~ 95%) within 4 and 9 days, respectively. Pore sizes in alginate matrices have previously been reported based upon quantitative diffusion studies by Choi et al. and Benerjee et al.[26, 27]; these studies suggest that the pore sizes for Ca-alginate are between 3 and 5 nm, much smaller than the radius of our USPIO nanoclusters (42 nm). Thus, one reason for delayed MEAN release rates from our microspheres could be that the nanoclusters block pores in the alginate matrix thus obstructing diffusion of drug from the microspheres. The PAA anionic polymer in the USPIO nanoclusters likely also contributes to the improved drug loading efficiency and delayed release kinetics. Many of the side chains of PAA on the USPIO nanoclusters lose their protons and acquire a negative charge. This makes PAAs polyelectrolytes with the ability to absorb and retain aqueous solutions including MEAN and swell to many times their original volume within the microspheres. Both transient surface absorption effects and aforementioned inherent physical barriers to diffusion should slow MEAN release rates from our alginate microspheres co-encapsulating USPIO nanoclusters. In addition, no significant degradation of the magnetic microspheres (0~5 wt % MC) was observed during 10 weeks. The results were matched with reported degradation rates of alginate microspheres that take several months (>12 weeks) to break down in the physiological fluid (J Mater Sci: Mater Med (2010) 21:2243–2251). The optimal composition for these microspheres is currently unknown; determination of effective doses (total volume of infused microspheres) and optimal MEAN release kinetics will require future pre-clinical and translational investigations. However, our current studies importantly demonstrate that drug loading and release rates can be readily altered by adjusting USPIO content during microfluidic fabrication processes.

McA-RH7777 Hepatoma Cell Growth Inhibition

These microspheres should permit selective image-guided transcatheter delivery of MEAN to liver tumors. This local delivery strategy should inherently permit a reduced dose of the drug to be administered when compared to systemic administration strategies while continuing to achieve potent levels of drug concentrations within the tumor tissues. However, controlling drug release rate from these microspheres will be important to avoid acute toxicities associated with rapid ‘burst’ release while also prolonging exposure of the targeted tumor tissues via sustained release of MEAN within the blood vessels that perfuse the tumor. The magnetic microspheres was tested to demonstrate cell inhibition effects by

the controlled drug release from the magnetic microspheres. We selected only a single composition to demonstrate the feasibility of eliciting potent cell inhibition with these MEAN eluting microspheres. For these studies, microspheres with 3wt% USPIO clusters were chosen as this composition represented a compromise between microspheres with 0 and 1%wt USPIO clusters with quite rapid drug release and 5wt% microspheres with much slower MEAN elution rates (only 30–40% drug eluted within 40 hrs). The HCC cell growth inhibition effects of free MEAN and MEAN-magnetic microspheres were investigated with exposure of the McA-RH7777 cell line to equivalent increasing doses (1.25 to 50 uM MEAN concentration) over a broad range of exposure intervals: 8, 24 and 40 hours. The only magnetic microspheres (0~5 wt% USPIO clusters) composed by the biocompatible alginate and iron oxide nanoparticles showed minimal toxicity (above 90 % cell viability) in a concentration range ~2 mg/ml. Both free MEAN and MEAN-magnetic microspheres demonstrated dose dependent cell growth inhibition effects (Fig. 9). However, minimal exposure time dependency was observed for cell growth inhibition measurements performed in samples exposed to free MEAN doses. These findings contrasted significantly with growth inhibition measurements performed for cell samples exposed to MEAN-magnetic microspheres; for the latter studies cell growth inhibition increased markedly with increasing exposure time, particularly for those samples treated with 12.5 to 50 uM doses. The latter findings can likely be attributed to the vast differences in exposure rates (i.e. cells exposed to the entire dose of free MEAN at onset rather than a continuously eluted MEAN dose from the microspheres).

FACS analysis was performed to confirm induction of apoptotic cell upon exposure to MEAN-magnetic microspheres. As seen in Fig. 10, exposure to MEAN-magnetic microspheres induced significant increases in McA-RH7777 apoptotic cell death. 24hrs of exposure to microspheres encapsulating MEAN doses of 12.5, 30 and 50 uM led to 15.2, 44.0 and 46.4% of the total cells entering either early or late stages of apoptosis. These results are consistent with previous studies demonstrating that MEAN inhibits tumor cell growth inducing apoptosis *in vitro* with potencies similar to the parental drug amonafide. Importantly, these studies also demonstrated that MEAN, initially encapsulated and then eluted from these magnetic alginate microspheres, maintains potency (cell killing ability) over a relatively long time period (up to 2 days).

Conclusion

Targeted transcatheter intra-arterial drug infusions can offer proven therapeutic benefits for patients with unresectable liver cancer. However, these approaches have generally resulted in only modest overall improvements in patient survival. Improved drugs and drug carriers for these loco-regional transcatheter approaches will be critical to more affectively treat this increasing patient population. For these purposes, we used microfluidics techniques to synthesize alginate microspheres encapsulating MEAN, a potent recently introduced DNA intercalator and USPIO nanoclusters. The resulting drug delivery platform was mono-disperse, microsphere sizes were readily controlled based upon channel flow rates during synthesis procedures, and drug release rates from the microspheres could be readily slowed with the introduction of USPIO nanoclusters. The MR relaxivity properties of the microspheres suggest the feasibility of *in vivo* imaging after administration and these microspheres exhibited potent therapeutic effects significantly inhibiting cell growth inducing apoptosis in hepatoma cells. The potential benefits of our magnetic microspheres drug delivery system are considerable because a sustainable release of chemotherapy over time could have a greater impact upon tumor kill. In addition, because the amount of chemotherapy loaded into the drug delivery carriers can be controlled, a more precise dose of chemotherapy could be delivered to the HCC tumors with MR image guidance. Future

pre-clinical animal model studies are now warranted to determine the in vivo efficacy of locally delivered MEAN-magnetic microspheres.

Acknowledgments

This work was supported by Basic Research Grant from ACS (American Cancer Society, Illinois chapter, ACS 279148) and by two grants R01CA159178 and RO1CA141047 from the National Cancer Institute. This work was supported by the Center for Translational Imaging at Northwestern University. Imaging work was performed at the Northwestern University Cell Imaging Facility generously supported by NCI CCSG P30 CA060553 awarded to the Robert H Lurie Comprehensive Cancer Center.

References

1. Llovet JM, Burroughs A, Bruix J. Hepatocellular carcinoma. Lancet. 2003; 362(9399):1907–17. [PubMed: 14667750]
2. Kew MC. Epidemiology of hepatocellular carcinoma. Toxicology. 2002; 181:35–38. [PubMed: 12505281]
3. Chow PKH, Tai BC, Tan CK, et al. High-dose tamoxifen in the treatment of inoperable hepatocellular carcinoma: A multicenter randomized controlled trial. Hepatology. 2002; 36(5): 1221–26. [PubMed: 12395333]
4. Lai CL, Wu PC, Chan GCB, Lok ASF, Lin HJ. Doxorubicin Versus No Antitumor Therapy in Inoperable Hepatocellular-Carcinoma - a Prospective Randomized Trial. Cancer. 1988; 62(3):479–83. [PubMed: 2839280]
5. Kettenbach J, Stadler A, Katzler IV, et al. Drug-loaded microspheres for the treatment of liver cancer: review of current results. Cardiovasc Intervent Radiol. 2008; 31(3):468–76. [PubMed: 18228095]
6. Moroz P, Jones SK, Gray BN. The effect of tumour size on ferromagnetic embolization hyperthermia in a rabbit liver tumour model. International Journal of Hyperthermia. 2002; 18(2): 129–40. [PubMed: 11911483]
7. Marelli L, Stigliano R, Triantos C, et al. Transarterial therapy for hepatocellular carcinoma: Which technique is more effective? A systematic review of cohort and randomized studies. Cardiovasc Intervent Radiol. 2007; 30(1):6–25. [PubMed: 17103105]
8. Biolato M, Marrone G, Racco S, et al. Transarterial chemoembolization (TACE) for unresectable HCC: A new life begins? European Review for Medical and Pharmacological Sciences. 2010; 14(4):356–62. [PubMed: 20496548]
9. Leichman CG, Tangen C, Macdonald JS, Leimert T, Fleming TR. Phase II trial of amonafide in advanced pancreas cancer. A Southwest Oncology Group study. Invest New Drugs. 1993; 11(2–3): 219–21. [PubMed: 8262735]
10. Ratain MJ, Mick R, Berezin F, et al. Phase I study of amonafide dosing based on acetylator phenotype. Cancer Res. 1993; 53(10 Suppl):2304–8. [PubMed: 8485716]
11. Scheithauer W, Dittrich C, Kornek G, et al. Phase II study of amonafide in advanced breast cancer. Breast Cancer Res Treat. 1991; 20(1):63–7. [PubMed: 1813070]
12. Liu YN, Norton JT, Witschi MA, et al. Methoxyethylamino-numonafide Is an Efficacious and Minimally Toxic Amonafide Derivative in Murine Models of Human Cancer. Neoplasia. 2011; 13(5):453–60. [PubMed: 21532886]
13. Norton JT, Witsch MA, Luong L, et al. Synthesis and anticancer activities of 6-amino amonafide derivatives. Anti-Cancer Drugs. 2008; 19(1):23–36. [PubMed: 18043127]
14. George M, Abraham TE. Polyionic hydrocolloids for the intestinal delivery of protein drugs: Alginate and chitosan - a review. Journal of Controlled Release. 2006; 114(1):1–14. [PubMed: 16828914]
15. Gombotz WR, Wee SF. Protein release from alginate matrices. Advanced Drug Delivery Reviews. 1998; 31(3):267–85. [PubMed: 10837629]
16. Kuo CK, Ma PX. Ionically crosslinked alginate hydrogels as scaffolds for tissue engineering: Part 1. Structure, gelation rate and mechanical properties. Biomaterials. 2001; 22(6):511–21. [PubMed: 11219714]

17. Lee KY, Mooney DJ. Hydrogels for tissue engineering. Chemical Reviews. 2001; 101(7):1869–79. [PubMed: 11710233]

18. Rowley JA, Madlambayan G, Mooney DJ. Alginate hydrogels as synthetic extracellular matrix materials. Biomaterials. 1999; 20(1):45–53. [PubMed: 9916770]

19. Zhang H, Tumarkin E, Sullan RMA, Walker GC, Kumacheva E. Exploring microfluidic routes to microgels of biological polymers. Macromolecular Rapid Communications. 2007; 28(5):527–38.

20. Fundueanu G, Constantin M, Ascenzi P. Poly(N-isopropylacrylamide-co-acrylamide) cross-linked thermoresponsive microspheres obtained from preformed polymers: Influence of the physico-chemical characteristics of drugs on their release profiles. Acta Biomaterialia. 2009; 5(1):363–73. [PubMed: 18723416]

21. Gonzalez-Rodriguez ML, Holgado MA, Sanchez-Lafuente C, Rabasco AM, Fini A. Alginate/chitosan particulate systems for sodium diclofenac release. International Journal of Pharmaceutics. 2002; 232(1–2):225–34. [PubMed: 11790506]

22. Kim HJ, Matsuda H, Zhou HS, Honma I. Ultrasound-triggered smart drug release from a poly(dimethylsiloxane)-mesoporous silica composite. Advanced Materials. 2006; 18(23):3083–88.

23. Ge JP, Hu YX, Biasini M, Beyermann WP, Yin YD. Superparamagnetic magnetite colloidal nanocrystal clusters. Angewandte Chemie-International Edition. 2007; 46(23):4342–45.

24. Zheng B, Georgakis GV, Li Y, et al. Induction of cell cycle arrest and apoptosis by the proteasome inhibitor PS-341 in Hodgkin disease cell lines is independent of inhibitor of nuclear factor-kappa B mutations or activation of the CD30, CD40, and RANK receptors. Clinical Cancer Research. 2004; 10(9):3207–15. [PubMed: 15131062]

25. Nisisako T, Torii T, Takahashi T, Takizawa Y. Synthesis of monodisperse bicolored janus particles with electrical anisotropy using a microfluidic co-flow system. Advanced Materials. 2006; 18(9):1152–56.

26. Banerjee A, Nayak D, Lahiri S. A new method of synthesis of iron doped calcium alginate beads and determination of iron content by radiometric method. Biochemical Engineering Journal. 2007; 33(3):260–62.

27. Choi NW, Cabodi M, Held B, Gleghorn JP, Bonassar LJ, Stroock AD. Microfluidic scaffolds for tissue engineering. Nature Materials. 2007; 6(11):908–15.

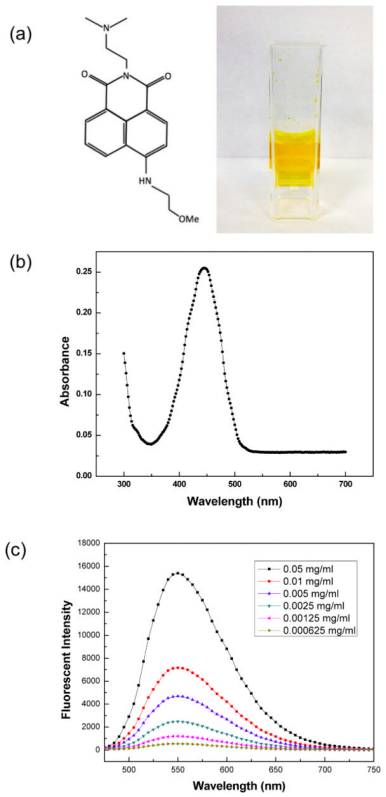

Figure 1.
Chemical structure and aqueous solution of MEAN (0.1 mg/ml) (a), absorption spectra (b) and fluorescent emission spectra (c) for MEAN.

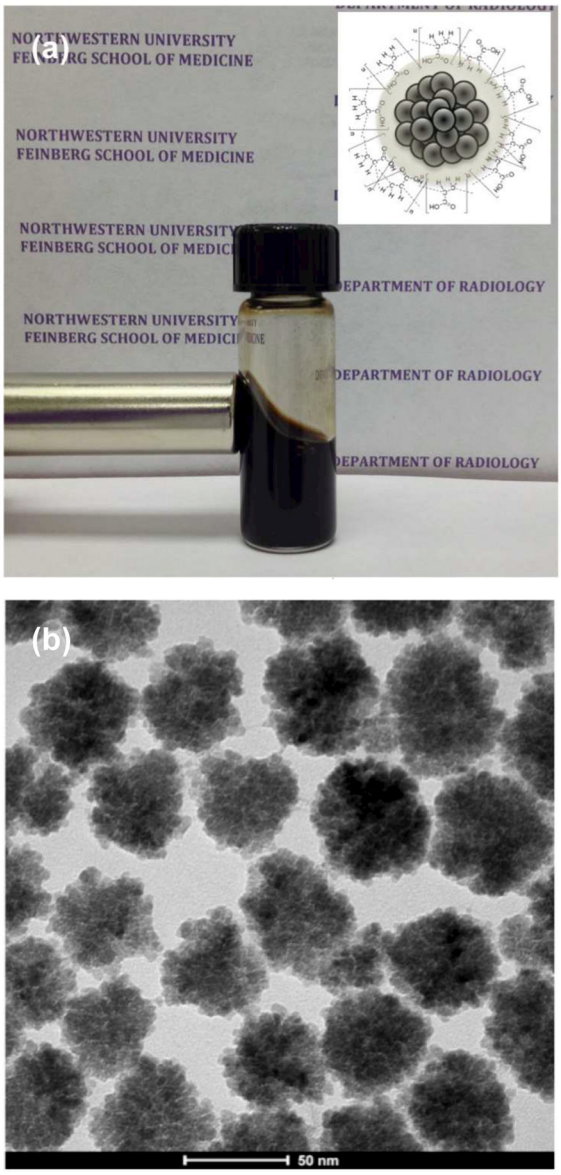

Figure 2.
USPIO clusters dispersed in aqueous solution (5 mg/ml) attracted by a permanent magnet (a) with inset depicting schematic structure of a USPIO nanocluster. TEM image of USPIO nanoclusters (b).

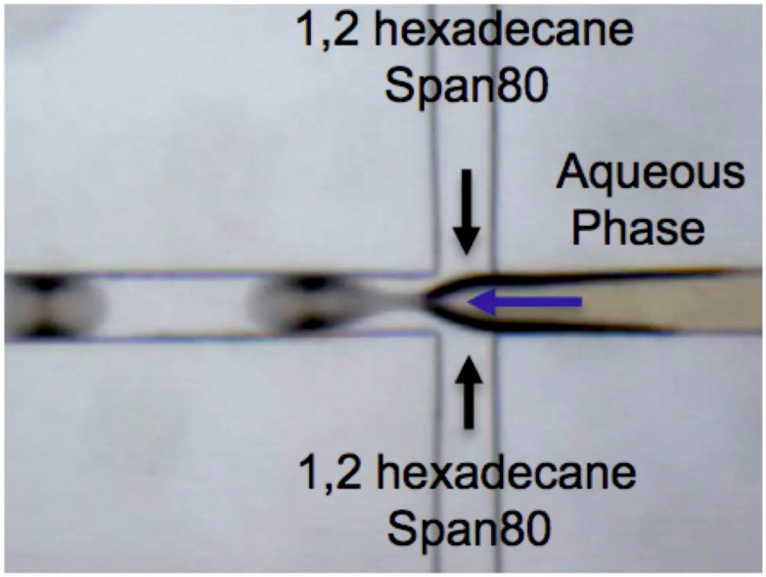

Figure 3.
Microscopy image of flow-focusing channel in Microfluidic PDMS device for generating microdroplets

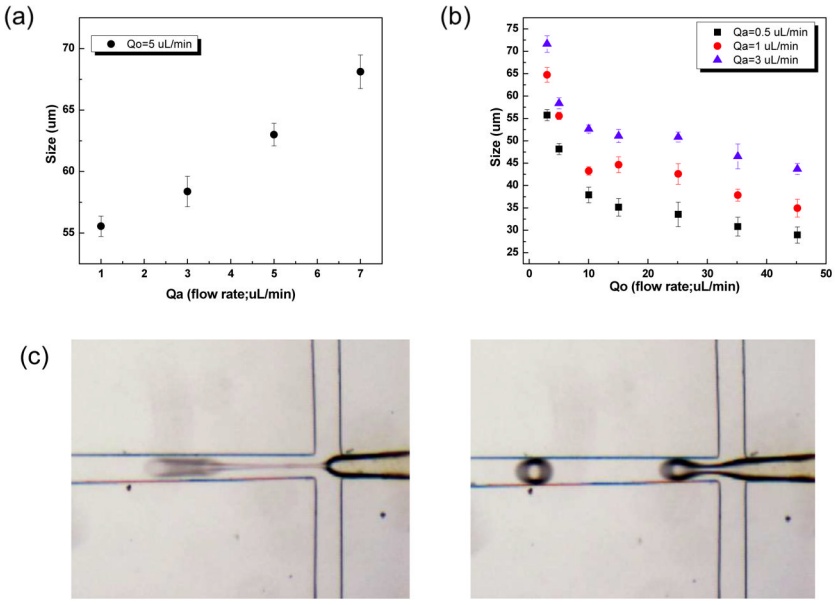

Figure 4.

Relationships between the droplet size and flow rates of dispersed and continuous phases. Size variation of dispersed phase droplets (mean diameter reported) as a function of flow rate, Q_c=5 ul/min and Q_d=1~7 ul/min (a). Size variation of dispersed phase droplets as a function of flow rate, Q_c=0.5~45 ul/min and Q_d=0.5, 1 and 3 ul/min and (b) Optical microscopy images showing the flowfocusing region generating droplets (c) (conditions: (left) Q_d =1 ul/min and Q_c=15 ul/min and (right) Q_d=1 ul/min and Q_c=5 ul/min, respectively)

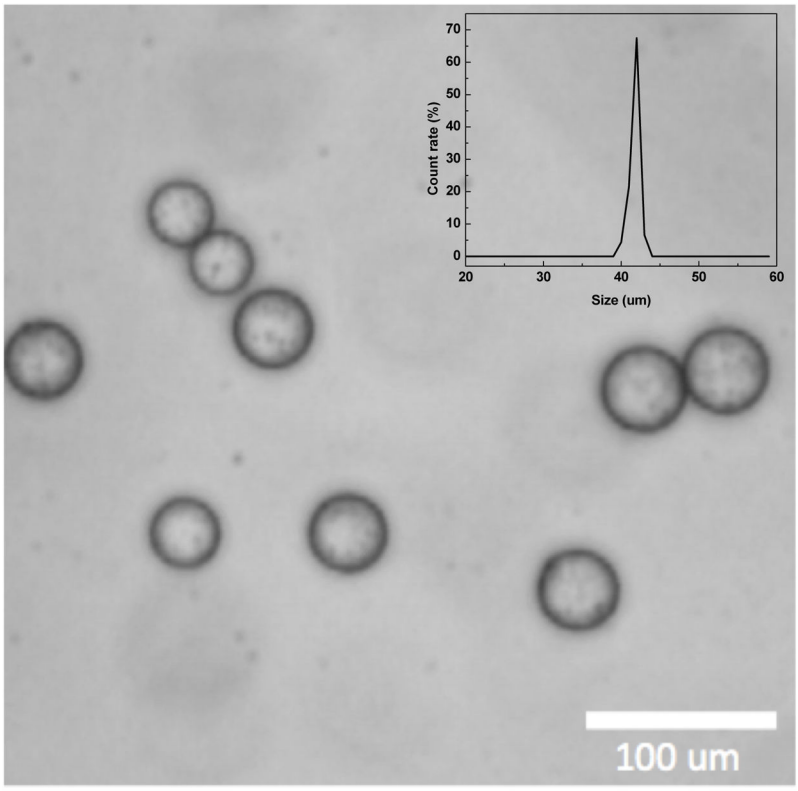

Figure 5.
Optical micrographs of MEAN-magnetic alginate microspheres fabricated with conditions Q_d =1 ul/min and Q_c=15 ul/min (Scale bar=100 um). Size distribution of these MEAN-magnetic microspheres (inset)

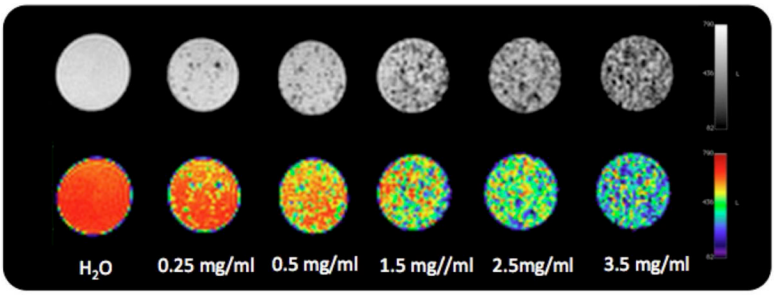

Figure 6.
T2*-weighted MR images and color map at TE= 6.4 ms showing the contrast effects in phantom signal intensity with increasing concentration of magnetic microspheres

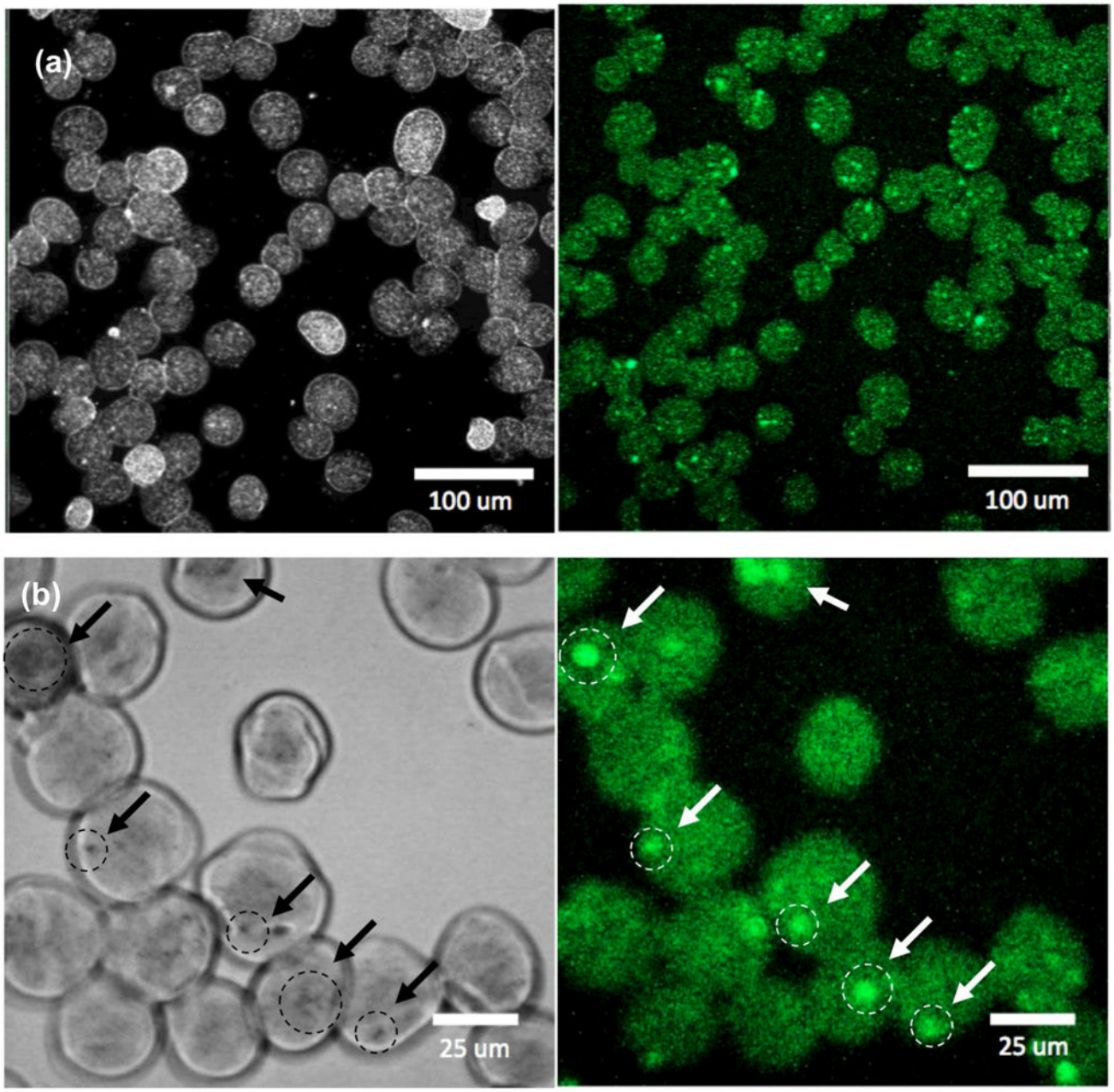

Figure 7.

Confocal microscopy (left) gray and (right) fluorescent images of MEAN loaded magnetic alginate microspheres ($\lambda_{excitation}$=445 and $\lambda_{emission}$=550 nm) ((a) low magnification and (b) high magnification, arrows indicate punctate regions of condensed USPIO clusters and intense fluorescent signal).

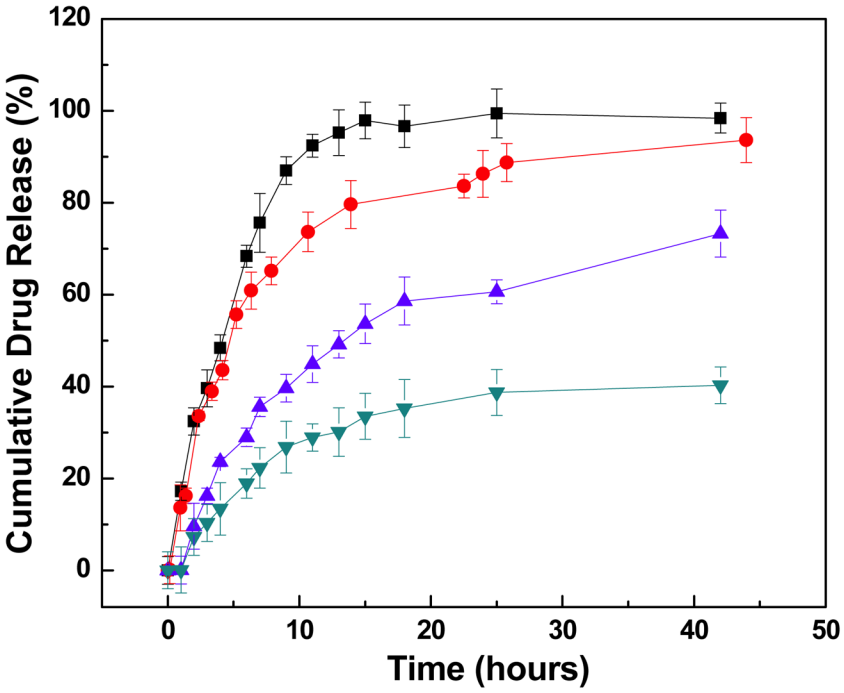

Figure 8.

In vitro drug release profiles for MEAN-magnetic microspheres incorporating increasing weight ratios of USPIO nanoclusters (0, 1, 3 and 5 wt%, top to bottom curves, respectively). The addition of USPIO nanoclusters slowed MEAN release rates.

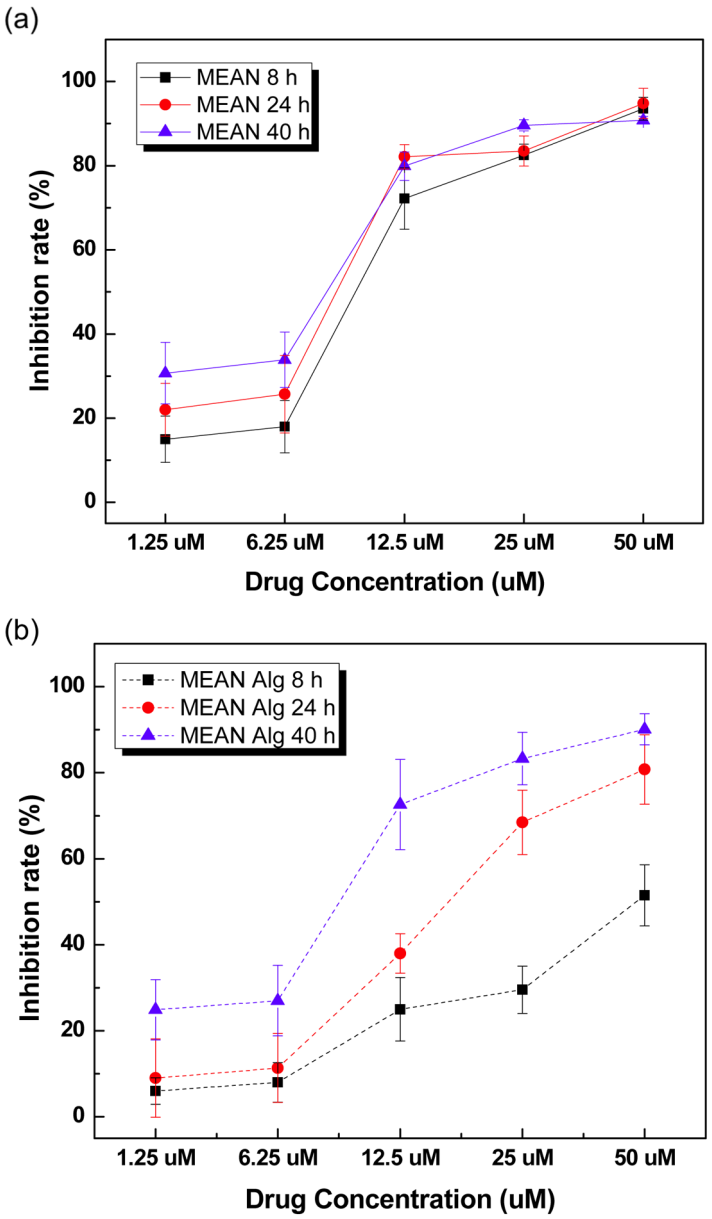

Figure 9.
McA-RH7777 cell growth inhibition effects for free MEAN (a) and MEAN loaded magnetic microspheres (3 wt% USPIO clusters) (b) at exposure times of 8, 24, and 40h with MEAN doses from 1.25 to 50 uM.

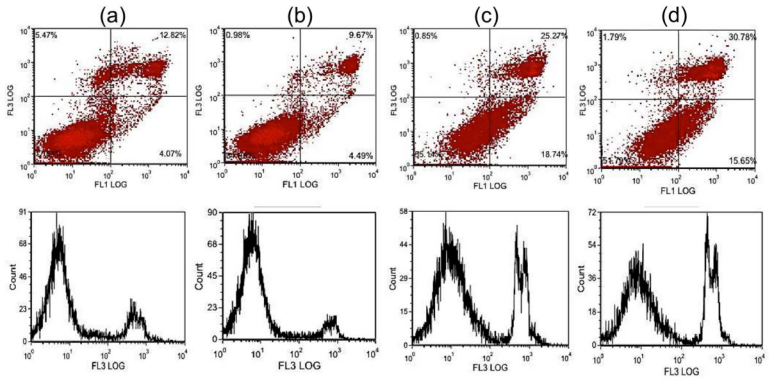

Figure 10.

Induction of apoptotic cell death upon exposure to MEAN-magnetic microspheres. FACS analysis using FITC annexin-V and propidium iodide staining: control (no exposure) (a), exposure to 12.5uM (b), 30uM (c), and 50uM (d) MEAN concentrations of MEAN-magnetic microspheres. Both flow cytometry (top) and associated histogram profiles (bottom) depict an increasing incidence of apoptotic cell death with increasing MEAN-magnetic microsphere dose.